Burnout resistance of concrete slabs: probabilistic assessment and global resistance factor calibration

Thomas Thienpont[1*], Ruben Van Coile[1], Robby Caspeele[1], Wouter De Corte[1]

[1] Department of Structural Engineering and Building Materials, Ghent University, Ghent, Belgium
Postal address: Technologiepark-Zwijnaarde 60, B-9052 Gent, Belgium

* Corresponding author: Thomas.Thienpont@UGent.be

Highlights

- Importance of considering a full burnout scenario in design for fire is illustrated
- Fragility curves for full burnout resistance of concrete slabs are presented
- Global resistance factor (GRF) as a safety format for reliability-based design
- Proposal of practical procedures for deterministic and GRF based design checks
- Example application of GRF-based full burnout fire design of a concrete slab

Abstract

Traditional prescriptive requirements for structural fire design do not explicitly ensure the load bearing capacity of the structure up to and including burnout. Therefore, a deterministic design method is presented, which enables to perform a quick check of the burnout bending resistance of a concrete slab exposed to a natural fire, and allows for the evaluation of (delayed) bending failure that can occur during or after the cooling phase, that would otherwise remain undetected. Subsequently, the influence of the inherent uncertainties associated with material properties and geometry on the design until full burnout is investigated. Reference fragility curves are presented and subsequently a global resistance factor (GRF) safety format for the fire design considering complete burnout scenarios is proposed. Application of the determined GRF allows for an explicit reliability-based design for fire exposed concrete slabs, without requiring the application of full-probabilistic methods. The concept is applied to simply supported reinforced concrete slabs and the calculated values are applicable to any compartment within the Eurocode parametric fire framework, through application of a scaling approach. The methods proposed in this contribution are intended as a stepping stone towards the development of GRF-based safety formats for more complex geometries and advanced numerical tools.

Keywords: Structural fire safety, Burnout resistance, Concrete slabs, Global resistance factor (GRF), Probabilistic assessment

1 Introduction

When employing traditional fire design, the primary qualification metric is the fire resistance *R*, which is expressed as the time a structural member can withstand exposure to a standardized time-temperature relation, such as the ISO 834 [1] or ASTM E119 [2], while maintaining its structural integrity and load bearing capacity. Herein, the temperature rise is defined as monotonically increasing, which is considered to mimic the post-flashover heating conditions of a severe fire [3]. This way of assessing the performance of fire exposed structures is adopted in many design practices and national codes (e.g. EN 1992-1-2:2004 [4], ASTM [2]). Although tests based on predefined time-temperature expressions provide a standardized way of comparing the performance of structural members exposed to fire, these methods fail to encompass information about the structural behaviour in a realistic fire scenario, which is not only characterized by a heating phase but also by a cooling phase, in which the temperature in the compartment decreases back to ambient conditions [5]. Therefore, considering a complete burnout scenario with a cooling phase in design also allows for the evaluation of (delayed) failure modes that would otherwise remain undetected [3,6]. More specifically in the case of reinforced concrete (RC) members, delayed failure can occur due to the fact that the maximum temperatures in the section can be reached a significant time after the beginning of the cooling phase [7,8]. Unlike in unprotected steel members, the relatively low thermal conductivity and high thermal capacity of concrete causes the inner layers of a section to heat up rather slowly. Consequently, the highest temperatures in the steel reinforcement can be reached long after the onset of the cooling phase. This is of major relevance for RC beams and slabs loaded in bending, which typically rely heavily on the steel tensile strength to maintain their load bearing capacities. Moreover, adopting the concept of designing structural members to survive the total duration of the fire until complete burnout provides clarity on the expected performance of the structure in case of fire (i.e. no loss of load-bearing capacity). This is very relevant in case of high rise buildings where the cost of a (partial) collapse would be enormous, or for irreplaceable assets such as precious cultural heritage. Moreover, this ensures the safety during fire brigades intervention and/or building inspection. Considering the above, a first objective of this article is to provide an easily applicable method to calculate the resistance until complete burnout for RC slabs.

The input values for the material properties and loads used in structural design are usually based on characteristic values, combined with partial factors, ensuring an appropriately low probability of failure, while limiting the complexity of the analysis. This approach is commonly referred to as being ‘‘semi-probabilistic’’ and provides a trade-off between simplicity and accuracy. For fire safety engineering applications however, no generally accepted safety targets and semi-probabilistic design methodologies currently exist [9]. Nonetheless, the structural fire engineering community has

demonstrated a growing interest in probabilistic methods in recent years [10–13], and there has been a call for the development of fragility curves for fire-exposed structural members, to support the application of probabilistic methods both in design as well as in standardization [14]. Therefore, a second objective of this paper is to develop reference fragility curves for bending capacity of simply supported RC slabs in a full burnout scenario.

Furthermore, most design guidance provides for simplified approaches whereby the design of structures is carried out on the level of individual members. This approach significantly simplifies design, but does not allow to take into account the specifics of a structure and the interaction between its components. Some of these interactions can significantly increase the fire performance, e.g. the formation of catenary action has been observed in composite floor systems [15–18], or beams in RC frames [19]. To overcome the limitations of single member design methods, non-linear Finite Element Model (FEM) analyses have become a commonly used tool for evaluating the response of concrete structures during or after exposure to fire [19–24]. The safety format to be applied with these non-linear numerical evaluations is currently unclear, and currently no generally accepted safety factor approach exists for reliability-based structural fire design [14]. In principle a full-probabilistic approach can be applied to incorporate uncertainties in structural fire design, using for example repeated sampling methods such as Monte Carlo simulations [25]. However, due to the highly non-linear behaviour of reinforced concrete and the time dependent exposure to fire, these design methods typically involve computationally demanding FEM evaluations. Consequently, the application of FEM for structural fire design requires the definition of a safety format which relies on a limited (ideally a single) evaluation of computationally expensive models. Various safety formats for non-linear FEM analyses have been proposed [26], such as partial factor methods, global safety formats and fully probabilistic methods. Cervenka [27] noted that the standard partial factor method cannot be applied to non-linear FEM calculations since the use of the extremely low design values for material properties may alter the structural response calculated by the non-linear FEM analysis. Cervenka concludes that a global resistance factor (GRF) is the most promising safety format to be used for non-linear fire design of concrete structures. A preliminary study into a GRF format for simply supported RC slabs was presented by Van Coile et al. [12]. Their investigation was based on studies by Allaix et al. [28] and Cervenka [27,29] amongst others, which propose to evaluate the global safety of a structure based on a single non-linear analysis using the mean values for the material properties and the geometry. The resistance obtained for this single non-linear evaluation constitutes a (first-order Taylor) approximation for the average resistance μ_R. This average resistance is divided by a GRF γ_R, to obtain the design value for the structural resistance R_d:

$$R_d = \frac{\mu_R}{\gamma_R}. \quad (1)$$

As the use of the GRF safety format to evaluate the safety of fire exposed concrete structures in a probabilistic risk assessment is being adopted in a growing number of publications [12,14,28–30], the last objective of this article is to explore the feasibility of this concept for simply supported RC slabs exposed to parametric fires until complete burnout. Application of the determined GRF will allow for an explicit safety-based design for fire exposed RC slabs, without requiring the application of full-probabilistic methods.

2 Fire resistance of RC slabs exposed to natural fire

In the following, an efficient evaluation procedure for determining the fire resistance of RC slabs exposed to natural fires is presented. First, the Eurocode parametric fire is summarily discussed and equivalency equations are presented which allow general application of results listed for a reference compartment. Subsequently, an analytical equation for the bending capacity during fire is introduced in Section 2.2. This evaluation is applied in Section 2.3 for the evaluation of the nominal fire resistance and burnout resistance (resistance verification for parametric fire exposure). Finally, an efficient evaluation procedure is proposed, to quickly check the design of a simply supported RC slab against full burnout.

2.1 Eurocode parametric fire curve

In the performance based design of RC structures exposed to fire, the use of natural (design) fire curves is desired in order to overcome the previously mentioned shortcomings related to the use of a traditional standard time-temperature curve. Analytical expressions for the time-temperature evolution in compartment fires can be found in Annex A of EN 1991-1-2:2002 [31] or in the German national annex DIN EN 1991-1-2:2010 [32]. Both fire curve definitions include a separate cooling phase which follows the heating phase, thus characterizing the fire up to full burnout of the compartment. In this article, the parametric fire curve from EN 1991-1-2:2002 is used, which is specified for compartments up to 500 m² floor area, with vertical openings only, and up to a compartment height of 4 m. This parametric fire curve has been adapted from derivations by Wickström [33] for the heat balance in a compartment during the heating phase. Unlike the prescriptive heating regimes prescribed in ASTM or ISO 834, the temperature development of the Eurocode parametric fire curve depends on the thermal and geometrical properties of the compartment, such as amount of combustibles, ventilation through vertical openings and thermal inertia of the enclosing walls, floor and ceiling. These parameters influence the rate at which the temperature in the compartment increases, which is expressed using a time-scaling factor Γ. A value Γ = 1 corresponds to a heating phase close to the ISO 834 standard heating curve, while Γ > 1 implies that higher temperatures are reached earlier, resulting in a fire which is colloquially ‘hotter’ than the ISO curve. The opposite applies for Γ < 1 [34]. Moreover, the Eurocode definition distinguishes two types of fires, i.e. fuel-controlled or ventilation-controlled. The nature of the fire is defined by the duration of the heating phase (DHP), which can be obtained using (2), with the DHP expressed in minutes and parameters listed in Table 1. Details on the calculation of these parameters are provided in Annex A of EN1991-1-2:2002.

$$DHP = 0.012\,\frac{A_f}{A_t}\frac{q_f}{O} \tag{2}$$

If the calculated DHP is shorter than a predefined limit value t_{lim}, the development of the fire is fuel controlled. In this case, the abundant supply of oxygen implies that the burning is limited by the heat release rate of the fuel itself, and not by oxygen supply. The heating phase duration then equals t_{lim}, accounting for a minimum time required to burn fuel. In the other case the fire is ventilation-controlled where, depending on the ventilation characteristics of the compartment, the heating phase lasts up to multiple hours. Typically, for dwellings and offices t_{lim} = 20 minutes is used, which corresponds to a fire with a medium growth rate, in accordance with EN 1991-1-2:2002, Annex A [31].

Table 1. Parameters of the Eurocode parametric fire curve, used in Eq. (2)

Parameter	Units
Opening factor O	$m^{1/2}$
Fire load density q_f	MJ/m²
Compartment floor area A_f	m²
Total compartment area A_t (floors, ceiling and walls)	m²

Figure 1 shows five Eurocode parametric fire curves and their corresponding Γ-values, together with the prescriptive ISO 834 heating regime. The parametric fires are expressed for a compartment with a floor area of 10x10 m^2, a height of 3 m, thermal inertia b = 1450 J/(m²$s^{0.5}$K), and fire load density q_f = 800 MJ/m². According to the definitions in the Eurocode, the curves with opening factors 0.02, 0.05, 0.1 and 0.15 are ventilation controlled fires, while the curve for O = 0.2 represents a fuel controlled fire. Note that the heating regime for Γ = 1 approximates the ISO 834 heating regime [33].

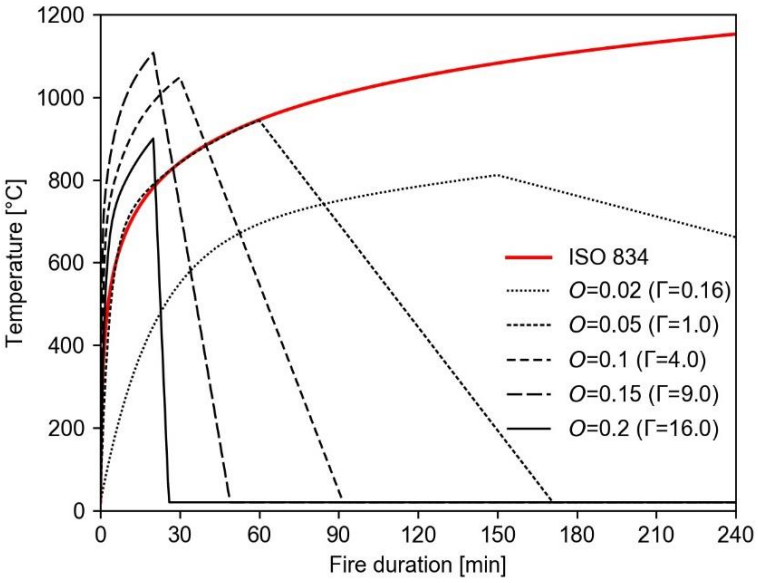

Figure 1: EN 1991-1-2:2002 parametric fire curves for q_f = 800 MJ/m² for different opening factors O, and ISO 834 standard fire curve.

Although the formulation of the Eurocode parametric fire curve is based on a large number of geometrical and thermal parameters, in essence it only has two degrees of freedom. All possible time-temperature relations can be expressed as a function of the Opening factor O and the fire load density per unit of floor area q_f. This implies that any parametric fire in a generic compartment with a given set of geometric and thermal properties is identical to the temperature-time curve in a reference compartment with an invariant geometry and invariant thermal properties when considering appropriate equivalent values for the fire load density $q_{t,eq}$ and opening factor O_{eq} for this equivalent compartment [7]. The equivalency formulas are presented in expression (3) and (4), in which b is the thermal inertia. The suffix '*eq*' refers to the equivalent compartment with fixed geometry and thermal inertia, while the other parameters refer to the generic compartment.

$$O_{eq} = O \cdot \frac{b_{eq}}{b} \tag{3}$$

$$q_{f,eq} = q \cdot \frac{A_f}{A_{f,eq}} \cdot \frac{A_{t,eq}}{A_t} \cdot \frac{b_{eq}}{b} \tag{4}$$

These equations are valid for both fuel and ventilation controlled fires. It should be mentioned that in the special case where the equivalent reference compartment parameters are $O_{eq} > 0.04$, $q_{t,eq} < 75$ MJ/m^2 and $b_{eq} < 1160$ J/(m^{2}s$^{0.5}$K), an additional parameter k needs to be taken into account as discussed in Hopkin et al. [34]. This issue can however be avoided by choosing the reference thermal inertia $b_{eq} \geq 1160$ J/(m^{2}s$^{0.5}$K). The above presented equivalency principles imply that the results presented further for RC slabs exposed to natural fires are applicable to any possible compartment, within the limits of the Eurocode parametric fire definitions.

2.2 Bending capacity of a fire exposed slab

The response of a simply supported RC slab, exposed from its bottom side to a natural fire scenario, is evaluated through a two-step procedure. First, the temperature development in the slab is calculated using a numerical 1D heat transfer model [7]. Herein, the entire cross-section is modelled as concrete with a moisture content of 1.5%, exposed to fire at the bottom. The temperature dependent material properties (lower bound thermal conductivity, specific heat and density) governing the heat transfer inside the concrete and the boundary conditions governing the heat transfer at the concrete-air interface are taken from EN 1992-1-2:2002 [4]. At the fire exposed side a concrete emissivity $\varepsilon_c = 0.7$ is used. The convective heat transfer coefficient $\alpha_{c,ISO} = 25$ W/m²K for ISO 834 fire exposures and $\alpha_{c,PF} = 35$ W/m²K for Eurocode parametric fire exposures. At the unexposed side, the convection coefficient is taken as $\alpha_c = 9$ W/m²K, assuming it contains the effects of heat transfer by radiation. Figure 2 shows the temperature evolution over time in a 200 mm thick concrete slab exposed to a natural fire with a 60 minute heating phase and subsequent linear cooling phase. The figure clearly

shows that the maximum temperature inside the solid slab (e.g. at depth = 50 mm) is reached a significant time after the onset of cooling. The highest temperatures (and corresponding lowest strength) in a rebar at that location are thus reached during (or after) the cooling phase, which illustrates the importance of taking into account a full burnout scenario in the fire resistance design of RC slabs.

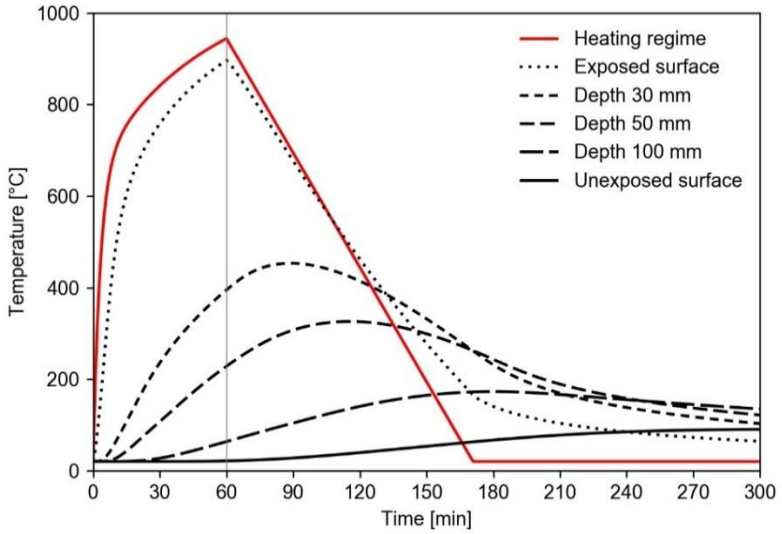

Figure 2: Temperature evolution in a 200 mm solid concrete slab, exposed from below to a Eurocode parametric fire with Γ = 1 and a heating phase of 60 minutes.

In a subsequent step, the temperature data generated with the heat transfer model are used as input to estimate the bending moment capacity $M_{R,fi,t}$ of a RC slab section with a single layer of bottom reinforcement using a simplified expression (5), as specified in Van Coile et al. [35].

$$M_{R,fi,t} = A_s k_{fy(\theta)} f_{y,20°C}(h-a) - 0.5\frac{\left(A_s k_{fy(\theta)} f_{y,20°C}\right)^2}{b f_{c,20°C}}, \qquad (5)$$

with A_s the area of reinforcement, k_{fy} the strength retention factor for reinforcement yield stress at temperature ϑ, $f_{y,20°C}$ the steel strength at 20°C, h the slab thickness, a the rebar axis distance (i.e. concrete cover + ½ rebar diameter), b the slab section width and $f_{c,20°C}$ the concrete compressive strength. The expression was validated against more detailed numerical simulations [13], and is based on the following assumptions:

- the concrete compressive area experiences only limited heating as the slab is exposed to fire from the bottom side only. Consequently, no reduction of the concrete compressive strength needs to be taken into account;
- in agreement with EN 1992-1-2:2004, the temperature ϑ of the rebars is assumed equal to that of the concrete at the rebar axis position;
- the influence of spalling on the structural fire resistance is not taken into account.

2.3 Fire resistance of a fire exposed slab

Applied to a simply supported slab loaded in bending, the European standard definition of the fire resistance of a component or structure yields equation (6). Herein, $M_{Rd,fi,t}$ is the design value of the bending moment resistance during fire exposure at time *t*. The design value for the bending moment induced by the load(s) $M_{Ed,fi}$ is assumed to remain constant for the entire duration of the fire exposure, in accordance with EN 1991-1-2.

$$M_{Rd,fi,t} \geq M_{Ed,fi} \text{ for } t \leq t_R \quad (6)$$

To express the ability of a structural member to survive a fire scenario until complete burnout, the Duration of Heating Phase burnout resistance (DHP_R) is used, i.e. a new metric proposed by Gernay & Franssen [5]. The DHP_R is defined as the shortest duration of the heating phase of a parametric fire that does not lead to eventual failure (possibly in the cooling phase) of the structural member under a certain design load. Consequently, for a fire with a longer duration of the heating phase, the member cannot survive the fire scenario until full burnout (assuming they have identical heating regimes, i.e. equal Γ values). Gernay and Franssen proposed to consider Γ = 1 as this allows a direct comparison of the DHP_R with the fire resistance R evaluated considering the ISO 834 standard fire exposure. The concept of the DHP_R is illustrated in Figure 3, which shows the evolution of the bending moment resistance $M_{Rd,fi,t}$ over time of a RC slab as defined in Table 2, exposed to three Eurocode parametric fires with Γ = 1 and a DHP of 110, 120 and 130 minutes respectively. In the scenario with DHP = 110 min, the bending moment resistance reaches a minimum value after 151 minutes, but the resistance stays well above the demand. Thereafter, due to cooling, the tensile strength in the steel reinforcement is (partially) recovered, and the slab is able to survive the complete burnout scenario. The recovery indicated in Figure 3 should be considered as indicative, as in real fire tests, irreversible damage phenomena can be observed in both concrete [36–38] and reinforcing steel [39–41]. The 120 minute DHP scenario follows an identical heating phase trajectory, but the onset of cooling starts 10 minutes later. Here, the minimum (i.e. most critical) value of the bending moment resistance is reached after 165 minutes, and stays just above the demand. If the DHP would be any longer, the slab would no longer fulfil the limit state design requirement as the bending moment resistance $M_{Rd,fi,t}$ becomes smaller than the demand $M_{Ed,fi}$. This failure is shown in Figure 3 for the case where DHP = 130 minutes. Thus, the slab defined in Table 2 has a burnout resistance DHP_R of 120 minutes.

To further illustrate the importance of considering a full burnout scenario, the bending moment resistance evolution over time for a ISO 834 standardized fire and a natural fire with Γ = 1 are compared in Figure 4. Following the definition in the Eurocode (6), the slab configuration in Table 2 has a fire resistance of 145 minutes. However, when taking into account a full fire scenario, the duration of the

heating phase should not exceed 120 minutes, otherwise a delayed failure is to be expected. In general, it can be concluded that the DHP_R is significantly shorter than the traditional fire resistance time t_R when the heating regimes are similar (i.e. for $\Gamma = 1$). Only for natural fires with a very low heating rate (e.g. the curve for $O = 0.02$ $m^{1/2}$ in Figure 1) the DHP_R can be longer compared to the traditional fire resistance, see for example [7].

Table 2. Properties of example RC slab

height h	width b	Rebar axis distance a	Area of reinforcement A_s	f_{ck}	f_{yk}
200 mm	1000 mm	35 mm	785 mm²	30 MPa	500 MPa

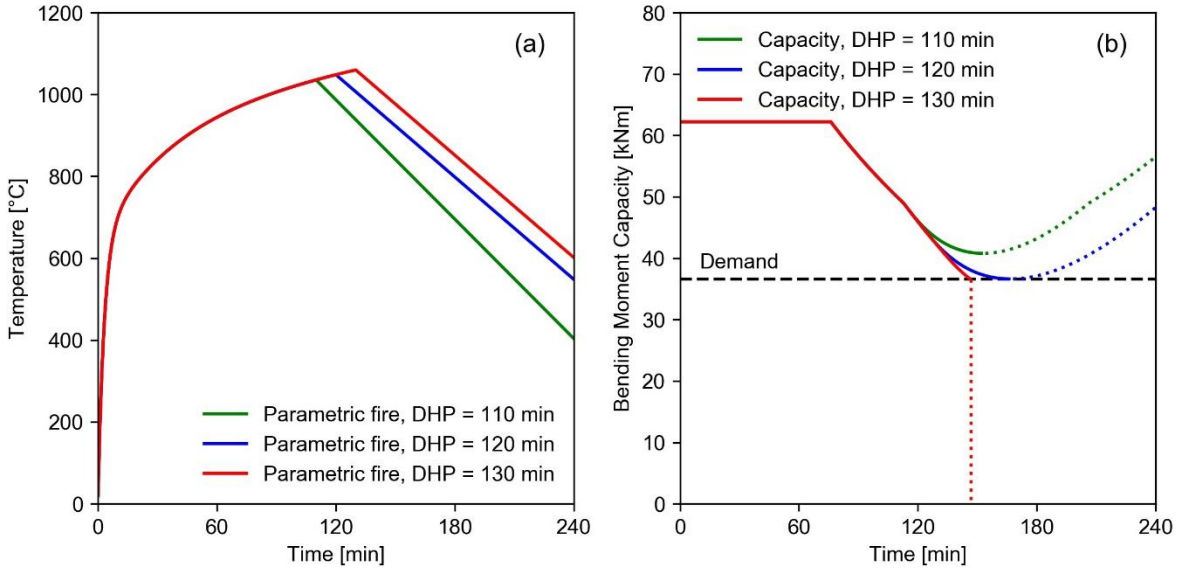

Figure 3: a) Time temperature curves for natural fires with $\Gamma = 1$ and DHP of 110, 120 and 130 minutes; b) evolution of bending moment capacity for the RC slab defined in Table 2, exposed to said natural fires.

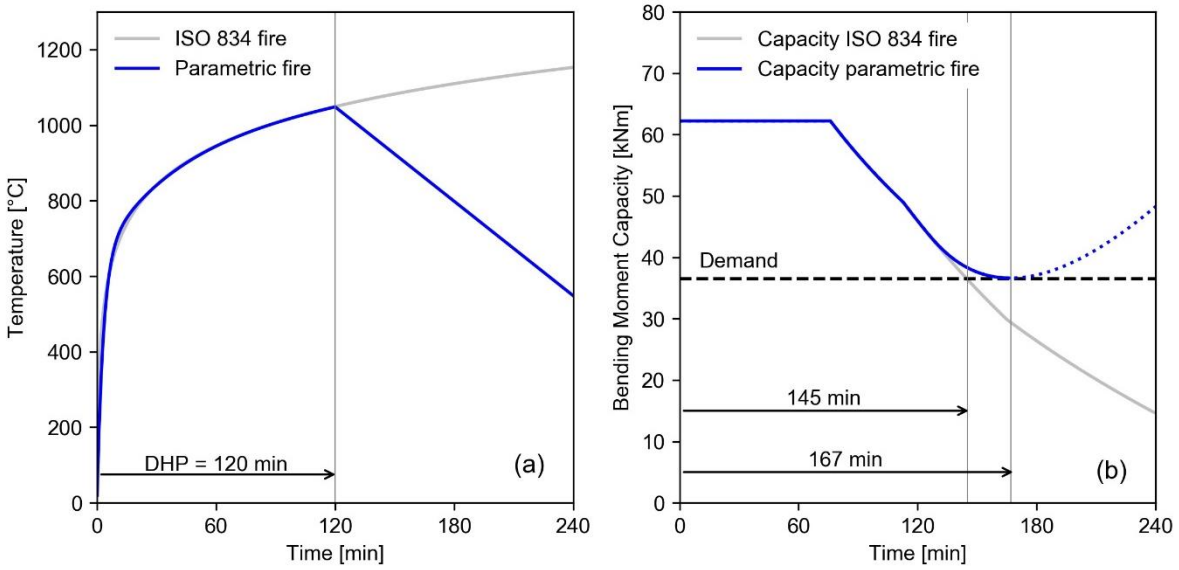

Figure 4: a) ISO 834 curve and a parametric fire with DHP of 120 minutes; b) evolution of bending moment resistance $M_{Rd,ISO}$ and $M_{Rd,PF}$ over time, reaching the design demand at respectively 145 and 167 minutes.

2.4 Efficient evaluation tool

The above presented method to demonstrate the bearing capacity of a RC slab considering complete burnout can be generalized using the equivalent compartment expressions and a regression model for the maximum rebar temperature Θ_{max}. The regression model relies on a large number of temperature calculations in a concrete slab. Through repeated calculation of the temperature development in a concrete slab, for a large number of possible combinations of Eurocode parametric fire curve parameters, i.e. opening factor O and fire load density q_f, the maximum rebar temperature Θ_{max} is obtained, taking into account a range of rebar axis distances a. Figure 5 shows the maximum rebar temperature in a 200 mm concrete slab at a depth a = 35 mm, calculated for a reference compartment, as defined in Table 3. Since slab height h has been shown to have very limited influence on the maximum rebar temperature when exposed to a parametric fire [7], the values for Θ_{max} in Figure 5 can also be used to estimate the maximum rebar temperature in slab with different heights. In the graph, a discontinuity can be observed, dividing the data points in two groups. The biggest data group, containing the highest temperature values, corresponds to ventilation controlled fires, whereas the smaller group represents the maximum rebar temperatures from fuel controlled fires. The gap between the two groups can be attributed to the definition of the Eurocode parametric fire, which contains a discontinuity in the region where it distinguishes between fuel controlled and ventilation controlled fires. This discontinuity however has no physical basis [42].

Combining all temperature data points, similar to those presented in Figure 5, over a range of rebar axis distances a, a regression model for predicting the maximum rebar temperature Θ_{max} for any Eurocode parametric fire is developed. Using a least-squares fitting algorithm [43], polynomial expressions for the maximum rebar temperature in both fuel and ventilation controlled fires are obtained, and presented in Annex A. Fuel and ventilation controlled fires are considered in separate models because of the discontinuity in the maximum temperatures. For the case of fuel controlled fires, a 4th degree polynomial allows for a very accurate prediction of the maximum temperature, with a maximum error of ± 5 °C. Similarly, a 3rd degree polynomial expression was found for ventilation controlled fires. The maximum error for this model is ± 20 °C, with the largest deviations occurring for fires with low values for both the opening factor O and fire load density q_f. Figure 6 presents the performance of both regression models where the dotted line represents perfect model behaviour. Furthermore, these figures show the mean average percentage error (MAPE) of the obtained regression models. When combined with the equivalence expressions for compartments, the obtained regression models allow for a very quick design procedure for a simply supported RC slab exposed to the parametric fire for a generic compartment within range of the Eurocode parametric fire curve parameters, as illustrated in Figure 7. Using the maximum rebar temperature and expression (5), the

burnout bending resistance $M_{Rd,fi}$ (i.e. the minimum value for the capacity during the entire natural fire) of a RC slab can be obtained in only a few iterations. This is demonstrated further in Section 5.

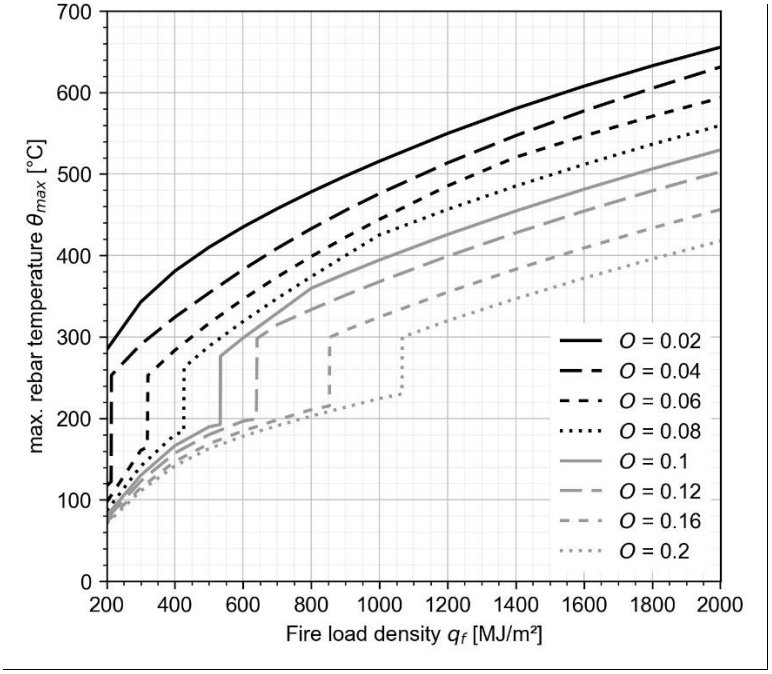

Figure 5: Maximum rebar temperature Θ_{max} in a 200 mm thick concrete slab, at depth a = 35 mm, as function of the opening factor O and fire load density q_f.

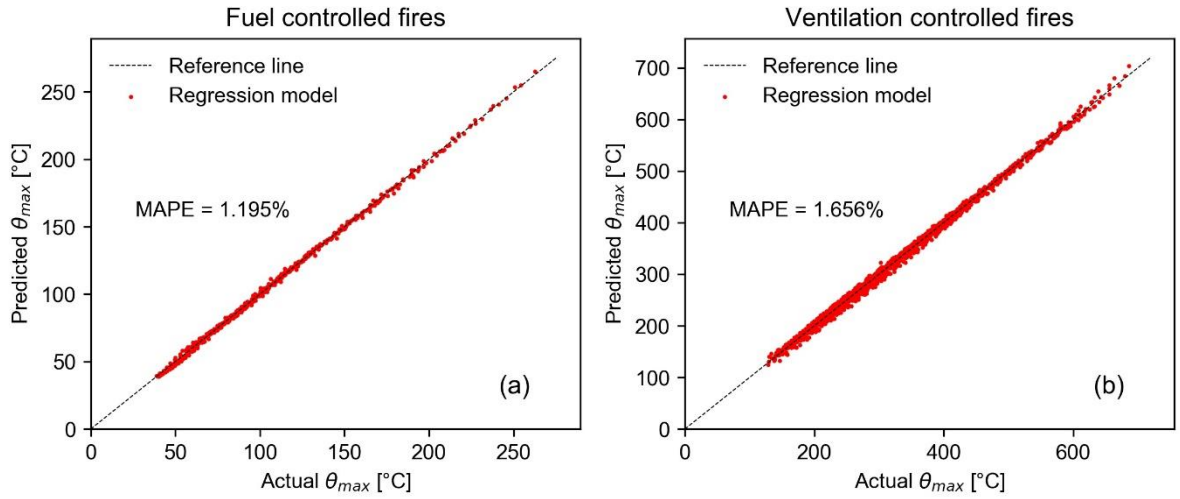

Figure 6: Performance of regression models for the maximum temperature Θ_{max} in a concrete slab at a certain depth, during a full burnout scenario.

Table 3. Properties of reference compartment for Θ_{max} calculations

length l_c	width w_c	height h_c	Thermal inertia b	Opening factor O	Fire load density q_f
10 m	10 m	3 m	1450 J/m²s$^{0.5}$K	variable	variable

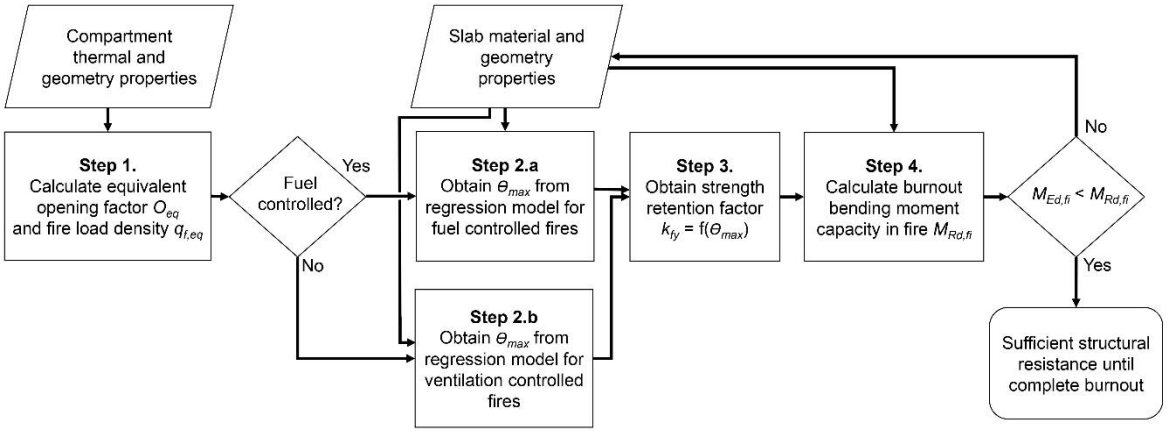

Figure 7: Deterministic design procedure for a RC slab exposed to a Eurocode parametric fire curve, to survive a complete burnout scenario.

3 Probabilistic evaluation of RC slab burnout resistance

3.1 Uncertainty

The preceding section clearly highlights the importance of taking into account the cooling phase of a compartment fire, to avoid delayed failure. Moreover, the evaluation tool presented in Section 2.4 shows that taking into account a more realistic fire scenario is fairly easy and only requires a limited number of steps. The proposed method is however based on deterministic modelling assumptions in accordance with the Eurocode design methodology (EN 1991-1-2:2002 and EN 1992-1-2:2004). Contrary to the Eurocode guidance for normal design conditions, the target safety level for accidental design situations is not well-specified. To overcome this issue, Van Coile et al. [44] proposed target safety levels for structural fire design, based on a simplified cost-optimization model. Alternatively, probabilistic methods are increasingly applied in fire safety engineering as a modification of more traditional design approaches, since these methods can more thoroughly assess the uncertainties associated with the design and explicitly demonstrate the attainment of an adequate safety level [9].

Taking into account uncertainty is indispensable for evaluating the structural fire response of RC members. For example, both steel and concrete have been experimentally observed to show a dispersal in the value of their respective structural strengths at room temperature, but more significant scatter is observed at the high temperatures typically associated with a building fire [45]. As concerns geometry, indicative values for the uncertainties on the dimensions of concrete members can be found in [46]. In the following, the fire load density is considered deterministic, as the current contribution is oriented to the uncertainty quantification of the structural resistance in relation to a known fire load.

To take into account the above uncertainties in the evaluation of the burnout capacity, first the probabilistic distribution of the bending moment resistance of RC slabs exposed to natural fire is obtained, and the influence of the opening factor and fire load density on these distributions is investigated. Taking into account the uncertain nature of the permanent and variable loads, a set of fragility curves are derived. Considering the previously presented equivalency expressions, these fragility curves are applicable for the entire range of Eurocode parametric fire parameters.

3.2 Probabilistic bending resistance of a fire exposed RC slab

To study the influence of the uncertainties related to the material properties and the geometry of fire exposed RC slabs, the distribution of the bending moment resistance is evaluated using Monte Carlo simulations. Figure 8.a and c shows the probability density function (PDF) and cumulative density function (CDF) for the bending moment resistance $M_{R,fi,t}$ of a RC slab, at ambient temperature (t_{fire} = 0), and considering exposure to three ISO heating regimes with varying duration. These graphs are obtained through repeated evaluation of Eq. (5) for 10^5 MC samples. In each sample, the slab

configuration is characterized by a vector X of randomly generated values of the probabilistic parameters listed in Table 4, with a mean rebar axis distance μ_a = 25 mm and reinforcement area A_s = 785 mm². By generating many variable vectors X, calculating $M_{R,fi,t}$ for each X, and analysing the results, the PDF and CDF of $M_{R,fi,t}$ are obtained [25]. Similar curves can be obtained for exposure to Eurocode Parametric fires, see Figure 8.b and d.

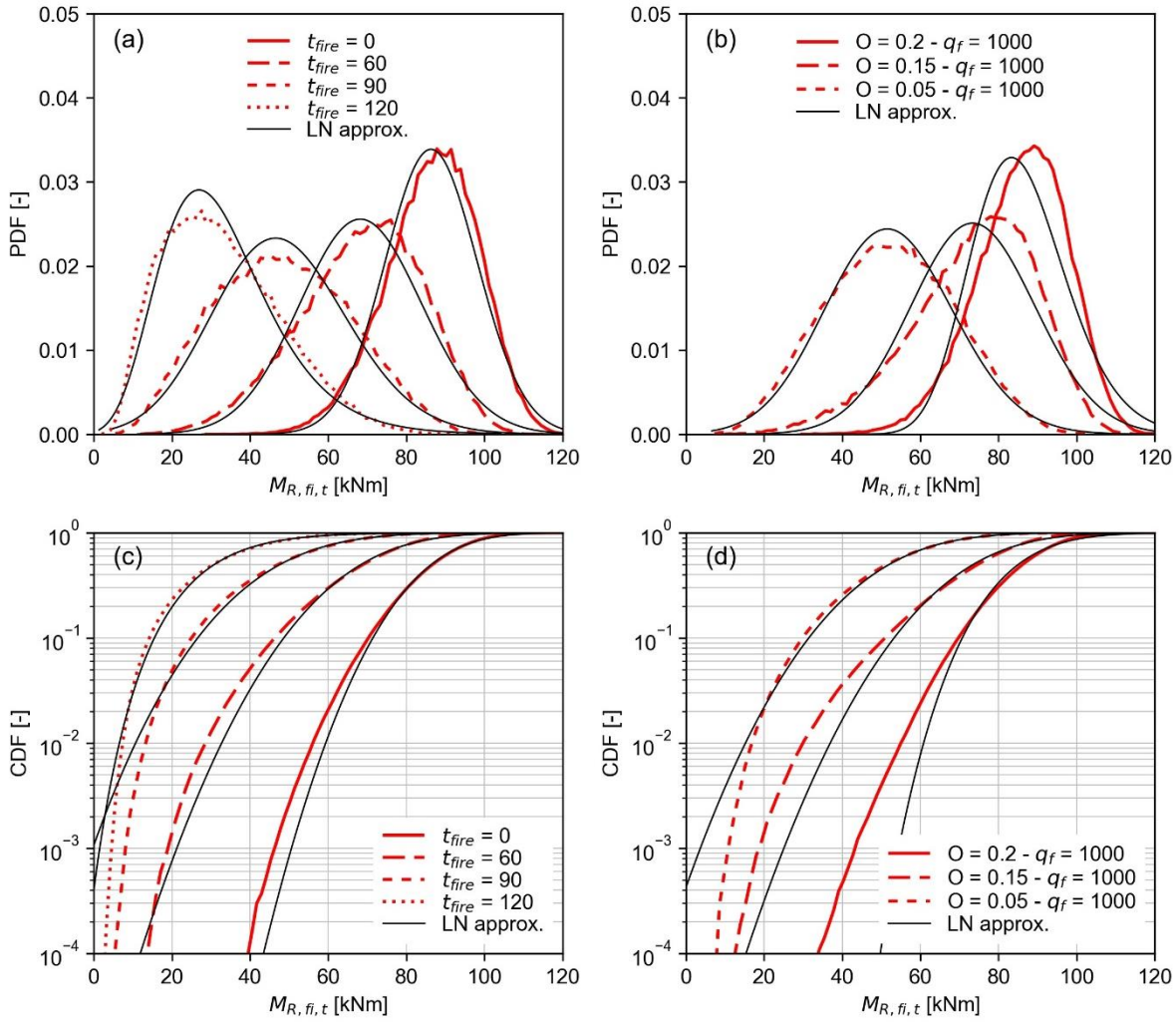

Figure 8: Bending moment capacity of a RC slab with mean rebar axis distance μ_a = 25 mm and parameters specified in Table 4, with lognormal fitting curves: a) PDF for $M_{R,fi,t}$ for exposure to ISO 834 fires; b) PDF for $M_{R,fi,t}$ for exposure to Eurocode parametric fires with varying opening factor; c) CDF for $M_{R,fi,t}$ for exposure to ISO 834 fires; d) CDF for $M_{R,fi,t}$ for exposure to Eurocode parametric fires with varying opening factor.

Table 4. Probabilistic models for RC slab variables

Property	Distribution	μ_X	COV_X	Reference
Concrete compressive strength $f_{c,20°C}$ at 20°C	lognormal	42.9 MPa (f_{ck} + 2σ)	0.15	[47]
Reinforcement yield stress $f_{y,(\Theta)}$ at Θ°C (variation incorporated in $k_{fy(\Theta)}$)	Deterministic*	560 MPa	-	-
Retention factor $k_{fy(\Theta)}$ for the steel yield stress at Θ°C	Logistic	temperature dependent	temperature dependent	[45]
Slab height h	Normal	200 mm	0.025 (σ = 5 mm)	[47]
Slab width b	Deterministic	1000 mm	-	-
Bottom reinforcement area A_s	Normal	1.02 A_s	0.02	[47]
Rebar axis distance a	Beta [$\mu \pm 3\sigma$]	μ_a	0.167 (σ_a = 5 mm)	[46,47]

* The temperature dependent reinforcement yield stress retention factor is modelled using the logistic model by [45]. This strength retention factor model already incorporates the variation in reinforcement yield stress at ambient temperatures. Therefore, the retention factor is combined with the mean yield stress at 20°C (deterministic value).

When lognormal curves are fitted to the obtained resistance distributions presented in Figure 8, the lognormal approximation is found to be an imperfect fit. In some cases, the lognormal approximation underestimates the frequency of low $M_{R,fi,t}$ values, while in other cases it gives a crude overestimation. For the Eurocode parametric fire with O = 0.15 and q_f = 1000, the lognormal approximation overestimates the 1% quantile by nearly 7 kNm, i.e. 23 %. Van Coile et al. [35] attributed this phenomenon to the variability in the rebar axis distance σ_a, and showed that the lognormal approximation is worse for larger σ_a or for lower rebar axis distances to the exposed surface.

In a full-probabilistic approach, variation in the concrete cover cannot be neglected, as several studies have emphasized the large influence of concrete cover on the structural performance of concrete structures during fire [30,48]. Since accurate lognormal fit curves cannot be obtained for the resistance distribution of RC slabs exposed to parametric fire, this paper presents a number of reference fragility curves for RC slabs exposed to parametric fire until complete burnout.

3.3 Failure probability of RC slabs exposed to natural fire

To demonstrate a high reliability with respect to the attainment of burnout resistance, the stochastic formulation for the bending capacity must be combined with appropriate load models and model uncertainties. The adequacy of the design can then be demonstrated by comparing the obtained probability of failure P_f to a specified target probability of failure $P_{f,t}$. Previous studies investigating the failure probability of concrete slabs [30,45] showed that in determining the capacity of the structure, the mechanical properties of steel at elevated temperatures cause large variance in the response.

For the case of a simply supported fire exposed RC slab subjected to bending, and considering a functional requirement of structural resistance up to and including burnout, the probability of failure

P_f is defined as the probability of the bending moment due to the load effect $M_{E,fi}$ exceeding the burnout (minimum) value of the bending moment capacity $M_{R,fi,t}$ of the slab:

$$P_f = P\left(K_R\, M_{R,fi,t} < K_E\left(M_G + M_Q\right)\right). \quad (7)$$

Herein, K_E and K_R are the model uncertainties for the load effect and the resistance effect respectively. The load effect is considered as a combination of the moment induced by the permanent load M_G and the moment induced by the applied variable load M_Q. The probabilistic models for the model uncertainties and load effects are given in Table 5. Herein, the probabilistic model for the moment induced by the variable load M_Q relates to an arbitrary-point-in-time load realization [49]. Moreover, the characteristic values M_{Gk} and M_{Qk} can be related by introducing the load ratio χ:

$$\chi = \frac{M_{Qk}}{M_{Gk}+M_{Qk}}. \quad (8)$$

The probability of failure P_f can be obtained in various ways, but the most straightforward method is to perform crude Monte Carlo simulations and evaluate the fraction of realizations for which the resistance effect is smaller than the load effect. Applying this technique, fragility curves can be obtained, which provide an easy way to evaluate the nominal load bearing capacity which satisfies a (maximum) target probability $P_{f,t}$ of not meeting the burnout resistance requirement. Figure 9 shows a number of fragility curves for the slab with properties specified in Table 2 and Table 4 with mean rebar axis distance μ_a = 35 mm and A_s = 785 mm², plotted as a function of the fire design utilization $u_{fi,,}$ which for a RC slab in bending is defined as the ratio between the design load $M_{Ed,fi}$ and design resistance $M_{Rd,fi}$ evaluated at the start of the fire exposure (i.e. at ambient temperatures, with k_{fy} = 1):

$$u_{fi} = \frac{M_{Ed,fi}}{M_{Rd,fi(20°C)}} = \frac{M_{Gk}+\psi_{fi}\,M_{Qk}}{M_{Rd,fi(20°C)}}. \quad (9)$$

The partial factors in the expression for $M_{Ed,fi}$ are omitted as they are equal to unity and the combination factor for the variable load ψ_{fi} = 0.3, i.e. the recommended value for residential and office buildings.

Additional fragility curves are provided in Figure 10 and Figure 11, illustrating the influence of the opening factor and fire load density on the probability of failure P_f. From the graphs it can be concluded that P_f increases significantly with decreasing opening factor O. Compartments with a small opening factor tend to lose less heat through the openings and thus reach higher temperatures, as can also be observed in Figure 6. Furthermore, the probability of failure also strongly depends on the fire load density and the load ratio, thus indicating the importance of considering these properties in fire design.

Table 5. Probabilistic models for load variables

Property	Distribution	μ_X	COV_X	Reference
Moment induced by the permanent load M_G	Normal	M_{Gk}	0.1	[49]
Moment induced by the variable load M_Q *(arbitrary point in time)*	Gamma	0.2 M_{Qk}	0.95	[49]
Model uncertainty for the load effect K_E	Lognormal	1	0.1	[49]
Model uncertainty for the resistance effect K_R	Lognormal	1.2	0.15	[47]

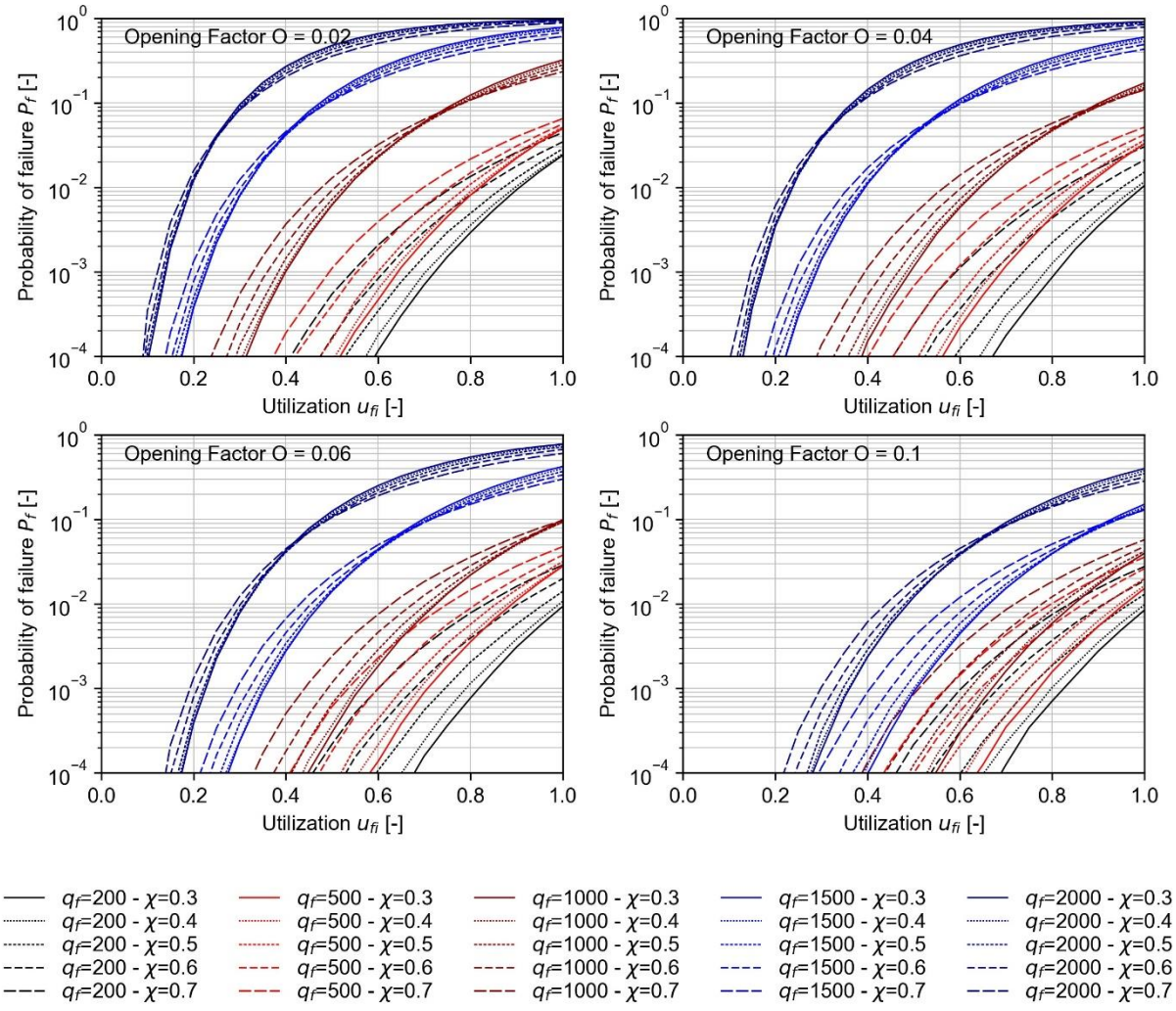

Figure 9: Fragility curves for RC slabs exposed to natural fires with varying opening factor O, and fire load density q_f

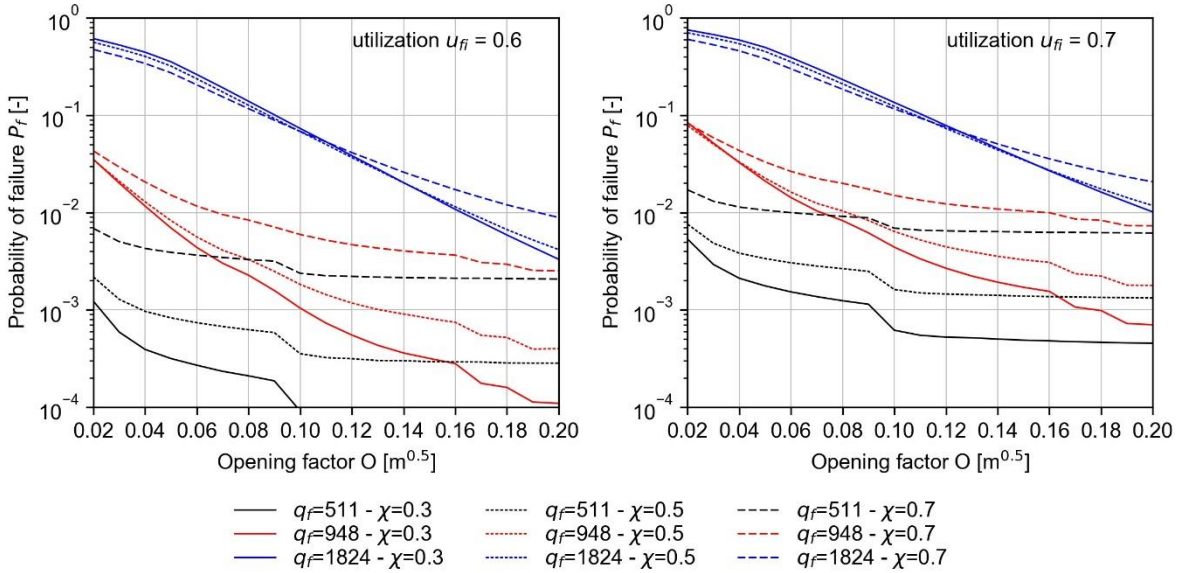

398

399 *Figure 10: Fragility curves for RC slabs exposed to natural fires, with varying opening factor O: a) utilization u_{fi} =*
400 *0.6; b) utilization u_{fi} = 0.7*
401

402

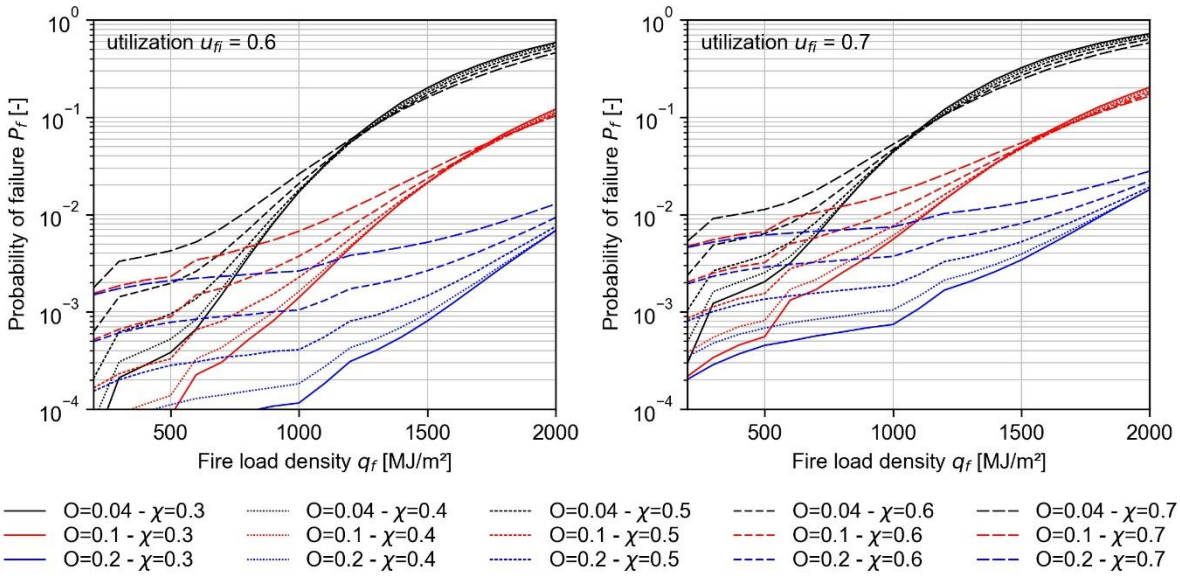

403

404 *Figure 11: Fragility curves for RC slabs exposed to natural fires, with varying fire load density q_f:*
405 *a) utilization u_{fi} = 0.6; b) utilization u_{fi} = 0.7*
406

4 Global resistance factor for RC slabs exposed to natural fire

As specified in the introduction, the global resistance factor (GRF) allows to perform a reliability-based evaluation, considering a single model evaluation using mean values for the stochastic variables. The design value for the resistance effect R_d is then obtained through Eq. (1). Applied to the situation of RC slabs subject to bending, the attainment of the target safety level is then confirmed through Eq. (10), where $\mu_{R,fi,t}$ is the evaluation of Eq. (5) considering the expected values for the stochastic variables.

$$\frac{\mu_{R,fi,t}}{\gamma_R} = M_{Rd,fi} > \mathrm{M}_{Ed,fi} = \mathrm{M}_{Gk} + \psi_{fi} M_{Qk} \tag{10}$$

In case the distribution of the bending resistance $M_{R,fi,t}$ can be accurately fitted with a lognormal distribution, the GRF γ_R can be approximated directly by Eq. (11), as applied in [12,14,27,28], with α_R the sensitivity factor of the resistance, V_R the coefficient of variation of the (bending) resistance, and β the target reliability index.

$$\gamma_R \approx \exp\left(\alpha_R V_R \beta\right) \tag{11}$$

However, as illustrated in the previous section, the lognormal distribution cannot be used to approximate the bending moment resistance distribution of RC slabs for natural fire exposure. Therefore, the simple approximation of the GRF using Eq. (11) is not appropriate, and an alternative calculation method is required [30]. To this end, a large number of Monte Carlo simulations and a full probabilistic analysis are used to directly calculate the design resistance $M_{Rd,fi}$. Dividing this value by the average resistance $\mu_{R,fi,t}$ immediately yields the GRF. By repeating this process for a large set of parameters, reference graphs for the GRF can be obtained for different target failure probabilities $P_{f,t}$.

Figure 12.a presents the calculated values of the GRF for the slab configuration in Table 2 exposed to several ISO fire durations, for a load ratio χ = 0.5. The obtained GRF are significantly larger than those listed in Van Coile et al. [12], confirming the need to consider the non-lognormal distribution of $M_{R,fi,t}$. After approximately 90 minutes of fire exposure, the value of GRF increases rapidly, to almost twice the value at room temperature (20°C), and slightly decreases after 210 minutes. Figure 12.b displays the GRF for a value of P_f = 0.001 and load ratios χ varying from 0.3 to 0.7. For short fire exposure times, the influence of the load ratio is rather small, but starts to increase after approximately 90 minutes.

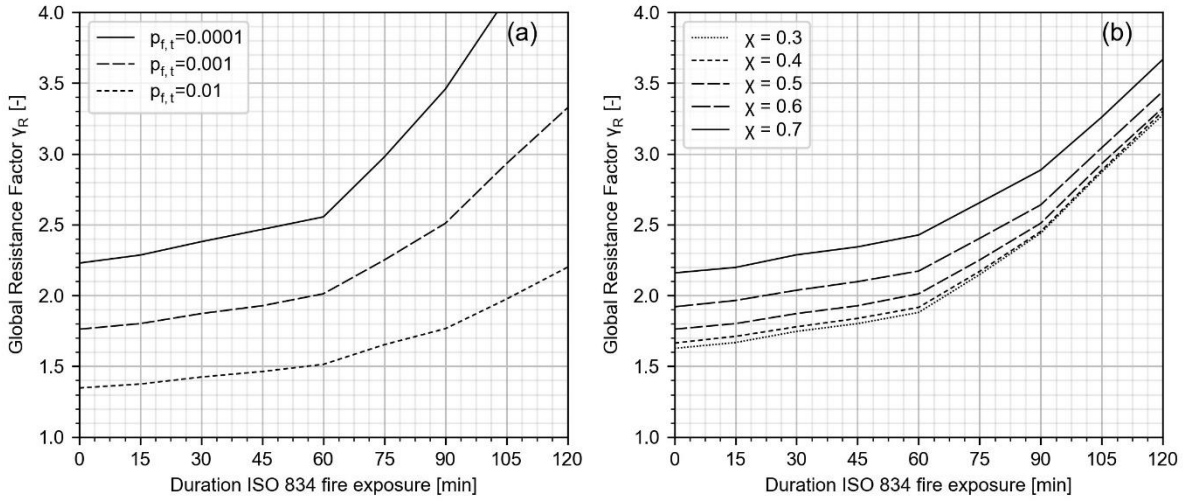

Figure 12: Global resistance factor values for the RC slab specified in Table 4, exposed to various ISO fires; a) for different value of probability of failure p_f and load ratio χ = 0.5, b) for different load ratios χ and p_f = 0.001.

In contrast to the prescriptive ISO fire curve, where the duration of the exposure t_f is the only variable influencing the fire scenario, for the Eurocode parametric fire curves at least two variables O and q_f need to be considered. This is illustrated in Figure 13 which shows the calculated values for the GRF for the slab in Table 4, for a wide range of O and q_f for a target failure probability $P_{f,t}$ = 0.001, a load ratio χ = 0.5, a combination factor ψ_{fi} = 0.3 and a rebar axis distance a = 0.035 m. The graph shows that γ_R has the highest values for compartment fires with limited ventilation (small O) and a large amount of combustible materials (large q_f), which also corresponds to the cases where the highest rebar temperatures Θ_{max} are attained (Figure 5). Moreover, coinciding with the discontinuity observed in the graphs for the maximum rebar temperatures, there is a discontinuity between the GRF values for ventilation controlled and fuel controlled fires, the latter values being slightly smaller. It can therefore be concluded that similar to the results for the ISO fire, higher GRF values are to be expected for more severe fires. To highlight some particular results, Figure 14 shows the GRF considering various target failure probabilities, for three opening factor values over a range of fire load densities q_f.

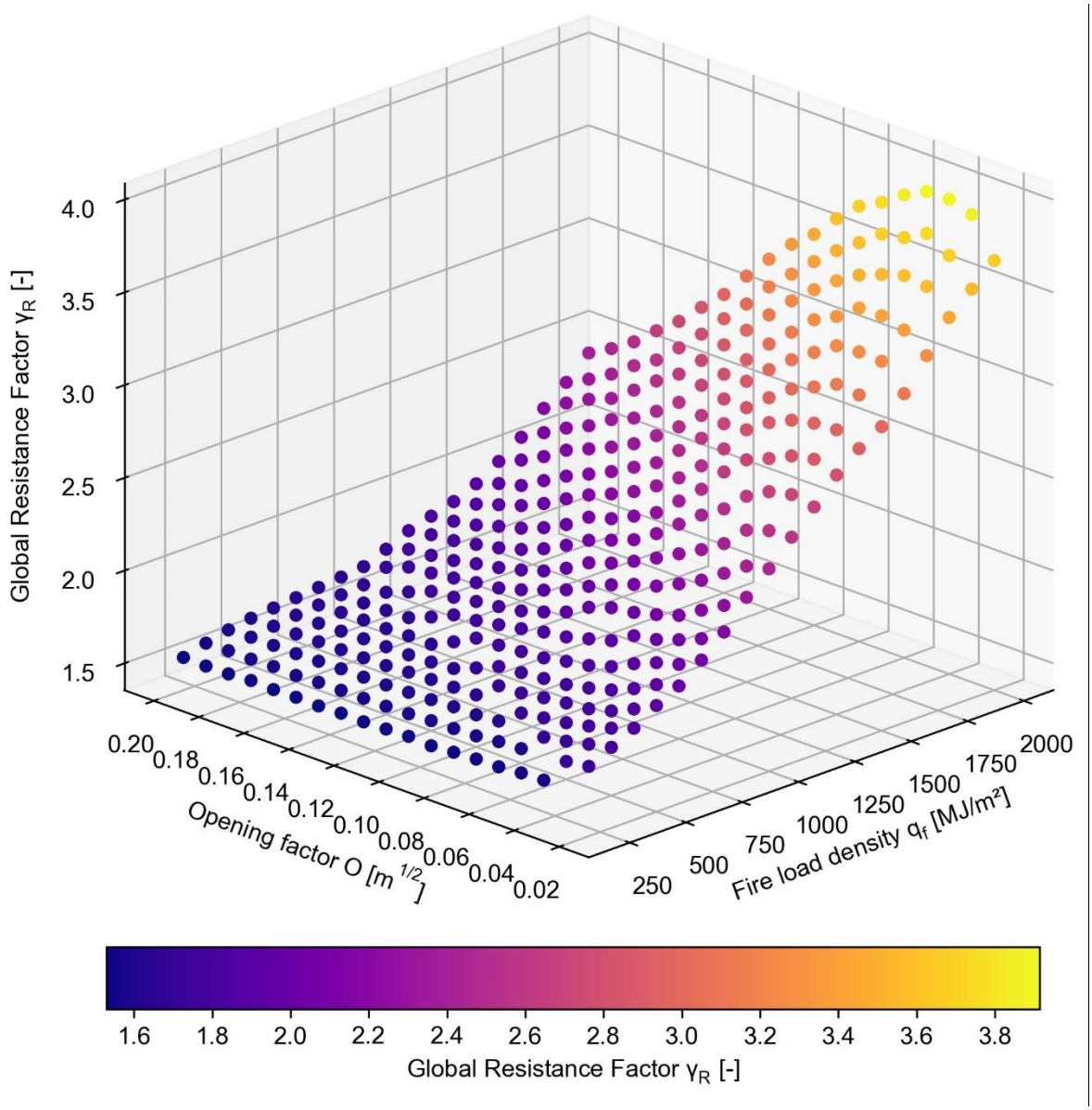

447

448 *Figure 13: Values for the global resistance factor for RC slabs exposed to natural fire for $P_{f,t}$ = 0.001 over a wide*
449 *range of opening factors O and fire load densities q_f*

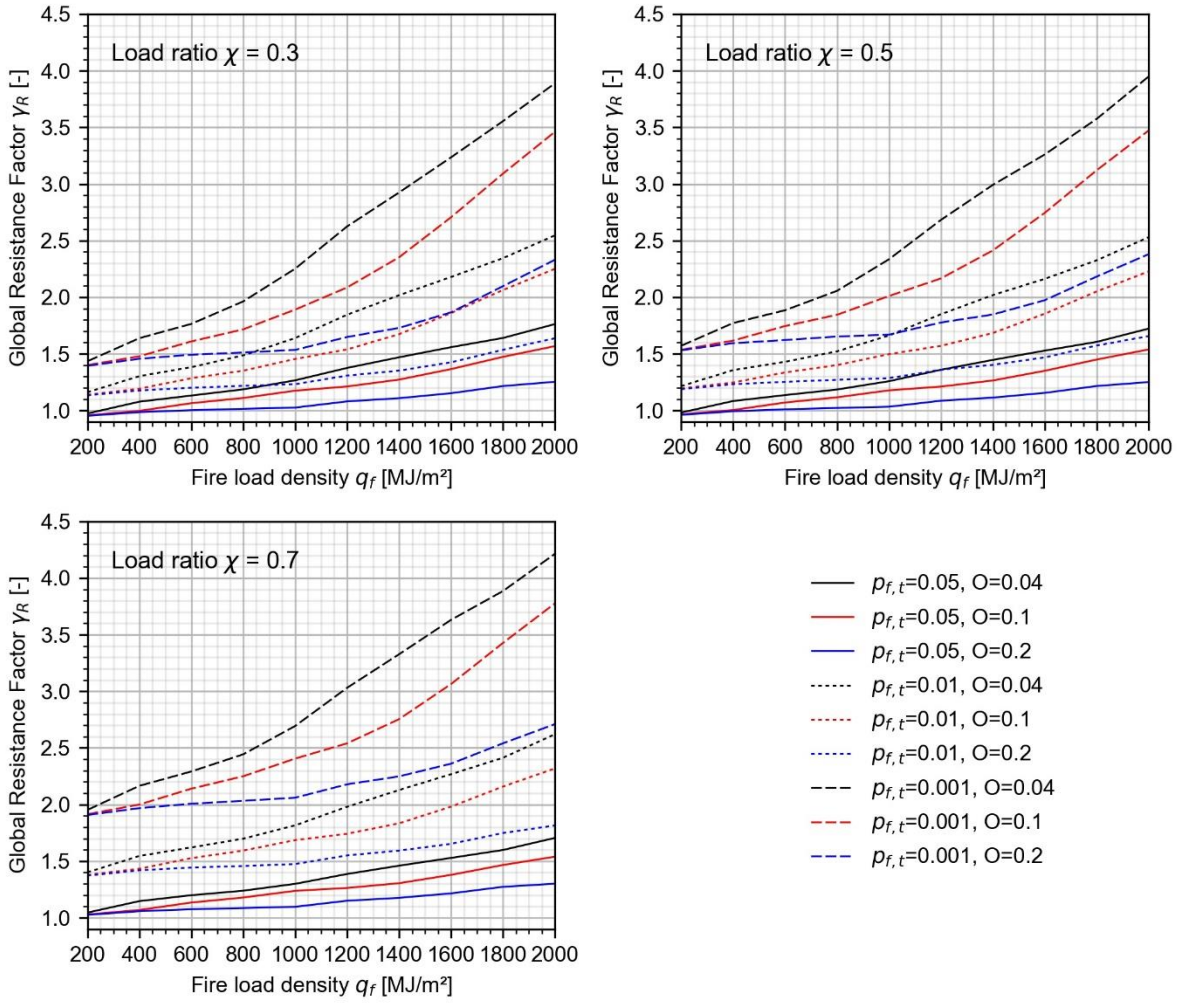

Figure 14: GRF for RC slabs exposed to natural fire, for various opening factors, load ratios and target failure probabilities, over a range of fire load densities.

4.1 Parametric study

To study the influence on the GRF of several geometry and load related parameters, a parametric study was conducted for a target probability of failure $P_{f,t}$ = 0.001, as illustrated in Figure 15. The graphs are calculated for two reference cases with fire load densities $q_{f,k}$ of 511 MJ/m² and 948 MJ/m², which in accordance with Annex E of EN 1991-1-2:2002 [31], corresponds to the 80% percentile of the recommended values for offices and dwellings respectively. The details and results from the study are summarized in Table 6. The last column of this Table, shows the relative deviation from the mean GRF value. This value corresponds to the worst pair of minimum and maximum values for the observed parameter pairs of O and q_f, divided by the mean GRF. In general, it can be concluded that the rebar axis distance, load ratio and reinforcement ratio have the highest influence on the GRF values, while concrete compressive strength (spalling not considered) and steel tensile strength seem to have no significant influence. Thus, in order to provide a simplified GRF based design tool, the influence of these parameters could be neglected.

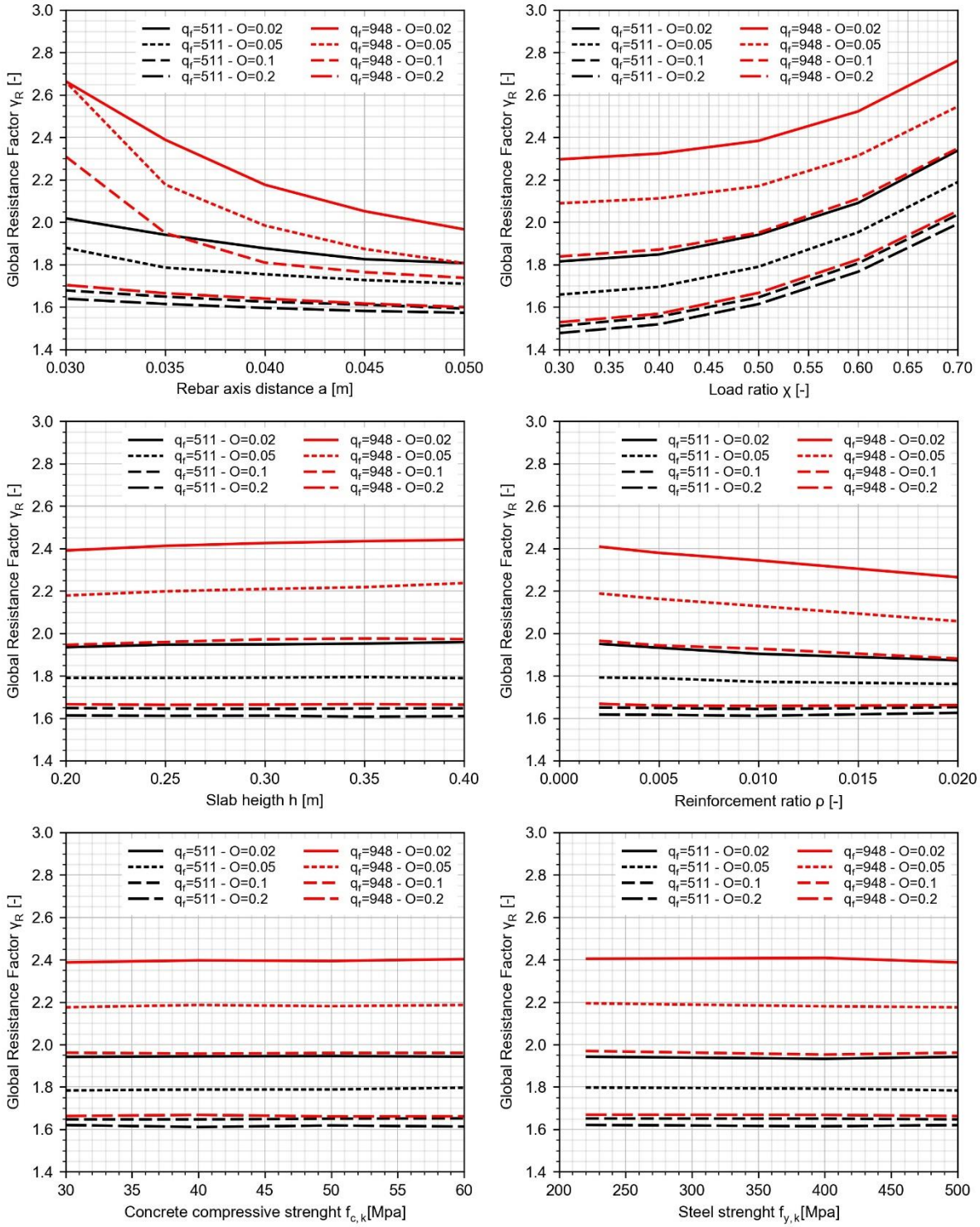

Figure 15: Influence of geometric parameters and material properties on the GRF for RC slabs exposed to natural fire: a) rebar axis distance; b) load ratio; c) slab height; d) reinforcement ratio; e) concrete compressive strength; f) steel tensile strength.

Table 6. GRF parameter study

Property	Investigated range	Influence on GRF	Max-Min /mean (%)
Rebar axis distance a	0.03 m - 0.05 m	Very large effect	79.47
Load ratio χ	0.3 - 0.7	Very large effect	17.56
Slab height h	0.2 m - 0.4 m	Very small effect	0.92
Reinforcement ratio ρ	0.2% - 2%	Small effect	5.83
Concrete strength f_{ck}	30 MPa – 60 MPa	Very small effect	0.26
Steel strength f_{yk}	220 MPa – 500 MPa	Very small effect	0.51

4.2 Efficient evaluation tool

By generating a set graphs as shown in Figure 14, for various values of the load ratio and concrete cover, the GRF can be very quickly estimated for a wide range of geometric and material parameters.

Using these graphs, the design procedure presented in Section 2.4 is further elaborated to provide for an explicit safety-based design for fire exposed RC slabs until full burnout, as illustrated in Figure 16. This is demonstrated further in the application example in Section 5.

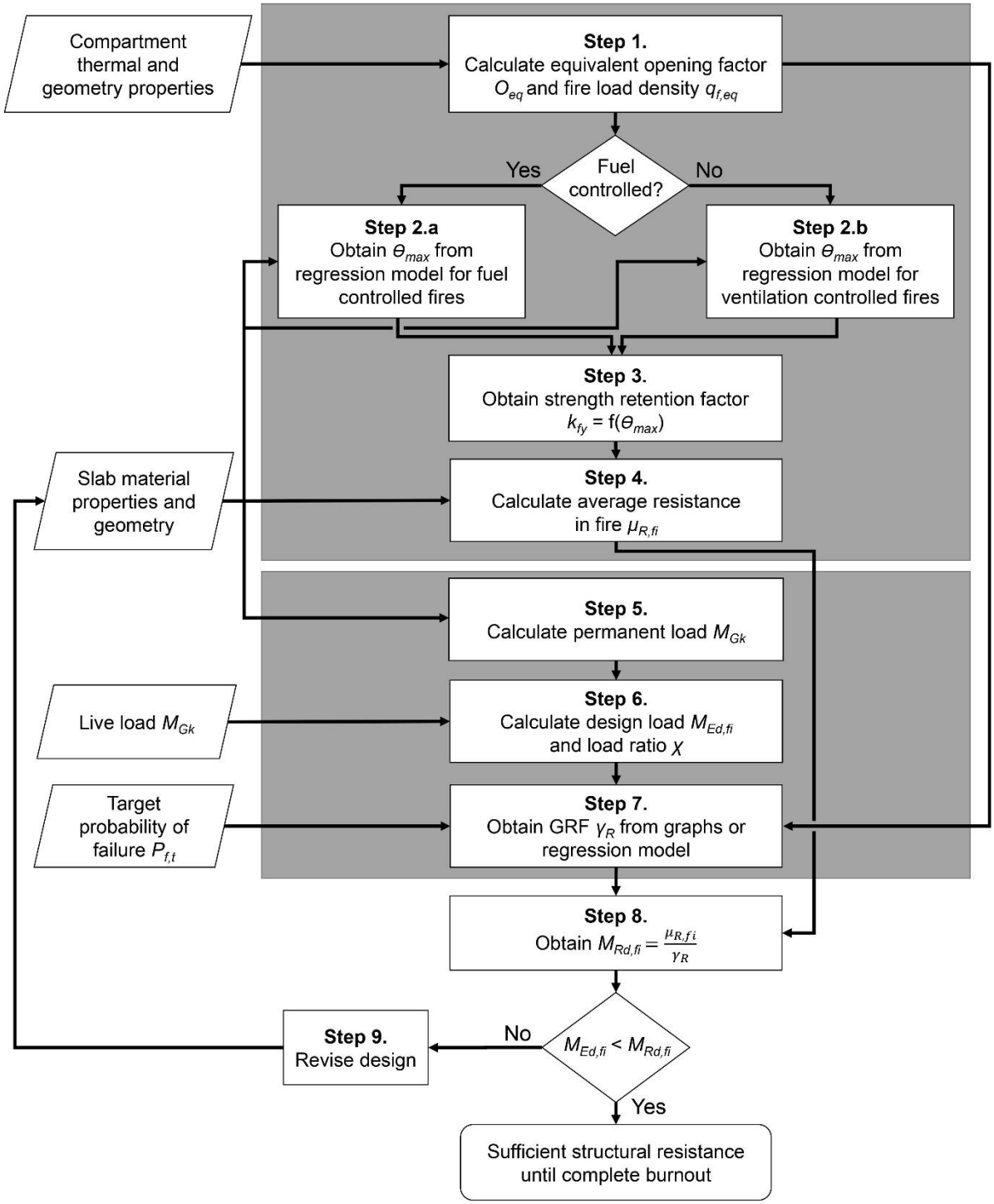

481

482 *Figure 16: Global resistance factor based design procedure for a RC slab exposed to a Eurocode parametric fire*
483 *curve, to survive a complete burnout scenario.*

484

5 Application example

In this section, an example analysis of a RC slab spanning a compartment in a residential building is conducted to assess the burnout resistance under natural fire conditions. The evaluation is done considering first the deterministic, and subsequently the GRF based design methods. The deterministic design check is compatible with the current Eurocode fire design methodology, but the obtained safety level remains unknown. When applying the GRF based design, a clear target (i.e. maximum allowable) failure probability is specified.

The geometric and material parameters for the compartment and the RC slab are presented in Table 7 and Table 8 respectively. Moreover, the bending moment $M_{Ed,fi}$ due to the transverse loads on the slab considered in this example is 51.7 kNm, corresponding to a load ratio χ = 0.3.

5.1 Deterministic design check

First, the nominal (design value) burnout bending moment resistance $M_{Rd,fi}$ is checked against the design load $M_{Ed,fi}$ considering a complete burnout scenario, using the compartment equivalence expressions (3) and (4) and design method as presented in Section 2.1. The equivalent reference compartment corresponding to the parameters in Table 7 is characterized by the parameters in Table 3, and O_{ref} = 0.1 $m^{1/2}$ and $q_{f,ref}$ = 1500 MJ/m². Using Eq. (2) yields a duration of heating phase DHP = 56.25 minutes, which corresponds to a ventilation controlled fire. The maximum rebar temperature Θ_{max} corresponding to O_{ref}, $q_{f,ref}$ and rebar axis distance a is obtained directly from Figure 5 or the surrogate model in Annex A, i.e. Θ_{max} = 470°C. Finally, the temperature dependent steel tensile strength retention factor k_{fy} = 0.848 corresponding to 470°C is obtained from the definition in EN 1992-1-2:2004, which is then substituted in (5) to obtain a burnout bending moment resistance $M_{Rd,fi}$ = 62.7 kNm. From the deterministic design check, it can be concluded that the slab defined in Table 8 is able to withstand a complete burnout scenario ($M_{Rd,fi} > M_{Ed,fi}$) and will not lead to delayed failure during or after the cooling phase.

5.2 GRF based design check

When the uncertainties in the material properties and geometry of the RC slab are to be taken into account explicitly, the safety of the design can be quantified through the pre-calculated GRF values and Eq. (1). First, the average resistance $\mu_{R,fi}$ = 71.1 kNm is obtained from the mean values μ_X for the material properties and the geometry. Herein, the deterministic value of the strength retention factor k_{fy} is obtained from the deterministic model presented in section 2.2. Then, from the previously calculated equivalency parameters O_{ref} = 0.1 $m^{1/2}$ and $q_{f,ref}$ = 1500 MJ/m², the GRF is taken directly from Figure 14. Considering a target failure probability $P_{f,t}$ = 0.01 a value γ_R = 1.77 is obtained. In the last step, the average resistance $\mu_{R,fi}$ is divided by the GRF, through which the design burnout bending

resistance $M_{Rd,fi}$ = 40.2 kNm is obtained. From this result, it can be concluded that design load $M_{Ed,fi}$ exceeds the design resistance, thus the slab design is deemed not to achieve the (maximum) target failure probability $P_{f,t}$ = 0.01. To confirm the accuracy of the GRF based design method, the design resistance $M_{Rd,fi}$ is compared to the value obtained from a full probabilistic evaluation. From $5 \cdot 10^6$ MC simulations $M_{Rd,fi,MC}$ = 41.8 kNm is obtained. It can therefore be concluded that the GRF based design method yields a safe (conservative) estimation of the design resistance.

Repeating the above evaluation for a higher value of $P_{f,t}$ = 0.05 results in a design resistance $M_{Rd,fi}$ = 71.1/1.32 = 53.9 kNm, from which it can be concluded that the slab with parameters in Table 7 will have a failure probability lower than 5%. This evaluation thus indicates that the deterministic design check results in a failure probability between 1% and 5%. The latter is confirmed with a full probabilistic evaluation ($5 \cdot 10^6$ MC simulations), which yields a failure probability p_f = 3.4%.

The example above shows that a GRF based design check which takes into account all material and geometry related uncertainties is easily applicable.

Table 7. Properties of example compartment

length l_c	**width w_c**	**height h_c**	**Thermal inertia b**	**Opening factor O**	**Fire load density q_f**
8 m	8 m	2.5 m	800 J/m²s$^{0.5}$K	0.055 m$^{1/2}$	840 MJ/m²

Table 8. Properties of example slab

Parameter	**Deterministic Calculation**	**Mean value evaluation ($\mu_{R,fi}$)**
Slab height h	0.2 m	0.2 m
Slab width w	1 m	1 m
Rebar axis depth a	0.035 m	0.035 m
Reinforcement ratio ρ	0.471% (Rebar ø12 – 120 mm)	0.481% (Rebar ø12 – 120 mm)
Concrete strength f_c	$f_{ck(20°C)}$ = 30 MPa	$f_{cm(20°C)}$ = 42,9 MPa
Steel strength f_y	$f_{yk(20°C)}$ = 500 MPa	$f_{ym(20°C)}$ = 560 MPa

6 Conclusions

Traditional design approaches where deterministic capacity assessments are combined with nominal time-temperature curves are insufficient for assessing the expected performance of structures exposed to real fires. To help address this, a number of innovations to the traditional approach have been presented, as applied to the bending resistance of simply supported RC slabs. Firstly, it was demonstrated that considering a full burnout scenario rather than a prescribed heating regime is of significant relevance, since the possibility of a delayed collapse cannot be neglected. Moreover, obtaining knowledge with regard to the structural response until complete burnout of a fire and beyond is essential as it benefits the safety of fire brigades and first responders, and enhances property protection and resilience of the built environment. In this regards, this research proposes a simple design tool, based on a surrogate model for estimating the maximum rebar temperature to quickly check whether a simply supported RC slab can withstand a fully developed Eurocode parametric fire until complete burnout.

The deterministic evaluation of the bearing capacity does not explicitly consider the many uncertainties associated with structures exposed to fire. Therefore, fragility curves are presented. These curves highlight the influence of the Eurocode parametric fire parameters on the load bearing capacity of RC slabs, indicating that the safety level obtained when applying deterministic design approaches is highly dependent on the compartment fire exposure characteristics. The load ratio (i.e. the ratio of the imposed load effect to the total load effect) is found to be of lesser importance, although not negligible. The analysis furthermore indicates that the bending capacity of concrete slabs during fire cannot readily be described by a traditional lognormal distribution.

To allow for a straightforward application of reliability considerations in the design of RC slabs for burnout resistance, a global resistance factor (GRF) approach is proposed. Application of a GRF allows to determine the design value of the resistance effect, i.e. the design value of the burnout bending moment capacity considering parametric fire exposure, considering only a single model evaluation with mean values for all stochastic input variables. The application of such an approach is of particular relevance for situations where the model evaluation is computationally expensive. Taking into account the calculated fragility curves, the required GRF for a specified target safety level in case of fire is numerically derived. Using these values as an input, a more elaborate design procedure for implementing a GRF based evaluation in a design is presented. The procedure illustrates how the application of the GRF allows for an explicit safety-based design for fire exposed concrete slabs, without requiring the application of expert probabilistic methods. Moreover, the calculated values are applicable to any compartment within the Eurocode parametric fire framework, through application

of a scaling approach. The methods proposed in this contribution are intended as a stepping stone towards the development of global resistance factor based safety formats for more complex geometries, considering partial or full structures rather than single members.

Acknowledgements

The authors wish to thank the Research Foundation of Flanders (FWO) for the financial support on the research project “Performance-based analysis and design for enhancing the safety of prestressed concrete hollow-core slabs in case of fire and unforeseen events”.

References

[1] Organization International for Standardization, ISO 834-1975. Fire resistance tests- elements of building construction, 1975.

[2] American Society for Testing and Materials, ASTM Standard methods of fire test of building construction and materials. Test Method E119a -08, West Conshohocken, PA, 2008.

[3] T. Gernay, Fire resistance and burnout resistance of reinforced concrete columns, Fire Saf. J. 104 (2019) 67–78. https://doi.org/10.1016/j.firesaf.2019.01.007.

[4] CEN, EN 1992-1-2. Eurocode 2 – design of concrete structures. Part 1–2: general rules – structural fire design, Brussels, 2004.

[5] T. Gernay, J.M. Franssen, A performance indicator for structures under natural fire, Eng. Struct. 100 (2015) 94–103. https://doi.org/10.1016/j.engstruct.2015.06.005.

[6] M. Salah Dimia, M. Guenfoud, T. Gernay, J.M. Franssen, Collapse of concrete columns during and after the cooling phase of a fire, J. Fire Prot. Eng. 21 (2011) 245–263. https://doi.org/10.1177/1042391511423451.

[7] T. Thienpont, R. Van Coile, R. Caspeele, W. De Corte, Comparison of fire resistance and burnout resistance of simply supported reinforced concrete slabs exposed to parametric fires., in: Proc. CONFAB 2019, London, 2019.

[8] H. Lakhani, A. Harapin, Behavior of concentrically loaded reinforced concrete columns under design fire, in: Proc. Fib Symp. 2019, 2019: pp. 598–604.

[9] R. Van Coile, D. Hopkin, D. Lange, G. Jomaas, L. Bisby, The Need for Hierarchies of Acceptance Criteria for Probabilistic Risk Assessments in Fire Engineering, Fire Technol. 55 (2019) 1111–1146. https://doi.org/10.1007/s10694-018-0746-7.

596 [10] M. Heidari, F. Robert, D. Lange, G. Rein, Probabilistic Study of the Resistance of a Simply-
597 Supported Reinforced Concrete Slab According to Eurocode Parametric Fire, Fire Technol. 55
598 (2019) 1377–1404. https://doi.org/10.1007/s10694-018-0704-4.

599 [11] I. Ioannou, W. Aspinall, D. Rush, L. Bisby, T. Rossetto, Expert judgment-based fragility
600 assessment of reinforced concrete buildings exposed to fire, Reliab. Eng. Syst. Saf. 167 (2017)
601 105–127. https://doi.org/10.1016/j.ress.2017.05.011.

602 [12] R. Van Coile, R. Caspeele, L. Taerwe, Global Resistance factor for concrete slabs exposed to fire,
603 in: M. Fontana, A. Frangi, M. Knobloch (Eds.), 7th Int. Conf. Struct. Fire, Zurich, 2012.

604 [13] R. Van Coile, Reliability-Based Decision Making for Concrete Elements Exposed to Fire, Ghent
605 University, 2015.

606 [14] R. Van Coile, D. Hopkin, N. Elhami-Khorasani, T. Gernay, Demonstrating adequate safety for a
607 concrete column exposed to fire, using probabilistic methods, Fire Mater. (2020) 1–11.
608 https://doi.org/10.1002/fam.2835.

609 [15] J.J. Chang, Computer simulation of hollowcore concrete floor systems exposed to fire,
610 University of Canterbury, 2007.

611 [16] N. Elhami Khorasani, T. Gernay, C. Fang, Parametric Study for Performance-Based Fire Design
612 of US Prototype Composite Floor Systems, J. Struct. Eng. (United States). 145 (2019) 1–15.
613 https://doi.org/10.1061/(ASCE)ST.1943-541X.0002315.

614 [17] C.G. Bailey, Membrane action of slab/beam composite floor systems in fire, Eng. Struct. 26
615 (2004) 1691–1703. https://doi.org/10.1016/j.engstruct.2004.06.006.

616 [18] L. Lim, Membrane action in fire exposed concrete floor systems, University of Canterbury, 2003.

617 [19] S. Albrifkani, Y.C. Wang, Behaviour of axially and rotationally restrained reinforced concrete
618 beams in fire, Eng. Struct. 213 (2020) 110572.
619 https://doi.org/10.1016/j.engstruct.2020.110572.

620 [20] A.M. Shakya, V.K.R. Kodur, Response of precast prestressed concrete hollowcore slabs under
621 fire conditions, Eng. Struct. 87 (2015) 126–138.
622 https://doi.org/10.1016/j.engstruct.2015.01.018.

623 [21] M.E. Baharudin, Modelling the structural response of reinforced concrete slabs exposed to fire:
624 validation , sensitivity and consequences for analysis and design, The University of Edinburgh,
625 2017.

626 [22] J. young Hwang, H.G. Kwak, Evaluation of post-fire residual resistance of RC columns
627 considering non-mechanical deformations, Fire Saf. J. 100 (2018) 128–139.
628 https://doi.org/10.1016/j.firesaf.2018.08.003.

629 [23] V. Albero, A. Espinós, E. Serra, M.L. Romero, A. Hospitaler, Numerical study on the flexural
630 behaviour of slim-floor beams with hollow core slabs at elevated temperature, Eng. Struct. 180
631 (2019) 561–573. https://doi.org/10.1016/j.engstruct.2018.11.061.

632 [24] S. Albrifkani, Y.C. Wang, Explicit modelling of large deflection behaviour of restrained reinforced
633 concrete beams in fire, Eng. Struct. 121 (2016) 97–119.
634 https://doi.org/10.1016/j.engstruct.2016.04.032.

635 [25] A.H.S. Ang, W.H. Tang, Probability concepts in engineering, 2nd ed., John Wiley & Sons, New
636 York, 2007.

637 [26] D.L. Allaix, V.I. Carbone, G. Mancini, Global safety format for non-linear analysis of reinforced
638 concrete structures, Struct. Concr. 14 (2013) 29–42. https://doi.org/10.1002/suco.201200017.

639 [27] V. Cervenka, Global Safety Format for Nonlinear Calculation of Reinforced Concrete, Beton- Und
640 Stahlbetonbau. 103 (2008) 37–42. https://doi.org/10.1002/best.200810117.

641 [28] D.L. Allaix, V.I. Carbone, G. Mancini, Probabilistic approach to the safety format for non- linear
642 analysis of concrete structures, in: Budelmann, Holst, Proske (Eds.), Proc. 9th Int. Probabilistic
643 Work., Braunschweig, 2011.

644 [29] J. Cervenka, V. Cervenka, Model Uncertainties and Global Safety Formats for Reinforced
645 Concrete Design by Numerical Simulation, NAFEMS World Congr. 2019. (2019).

646 [30] T. Thienpont, R. Van Coile, W. De Corte, R. Caspeele, Determining a Global Resistance Factor
647 for simply supported fire exposed RC slabs, in: Proc. Fib Symp. 2019, Krakow, 2019: pp. 2191–
648 2197.

649 [31] CEN, EN 1991-1-2. Eurocode 1: actions on structures – Part 1–2: general actions – actions on
650 structures exposed to fire., Brussels, 2002.

651 [32] DIN, EN 1991-1-2/NA National Annex - National determined parameter – Eurocode 1: Actions
652 on structures – Part 1-2: General actions – Actions on structures exposed to fire. Deutsche
653 Norm, 2010.

654 [33] U. Wickström, Application of the Standard Fire Curve for Expressing Natural Fires for Design
655 Purposes, in: Fire Saf. Sci. Eng., ASTM International, 100 Barr Harbor Drive, PO Box C700, West

656 Conshohocken, PA 19428-2959, 1985: pp. 145–159. https://doi.org/10.1520/STP35295S.

657 [34] D. Hopkin, R. Van Coile, C. Hopkin, K. Lamalva, M. Spearpoint, C. Wade, The Constraint: Design
658 Fires, in: Handb. Struct. Fire Eng., Springer (in press), n.d.

659 [35] R. Van Coile, R. Caspeele, L. Taerwe, The mixed lognormal distribution for a more precise
660 assessment of the reliability of concrete slabs exposed to fire, in: Safety, Reliab. Risk Anal., CRC
661 Press, 2013: pp. 2693–2699.

662 [36] G.A. Khoury, Y. Anderberg, K. Both, J. Fellinger, N. Høj, C. Majorana, Fib bulletin 38: Fire design
663 of concrete structures—materials, structures and modelling, state-of-the art report, 2007.

664 [37] Y.H. Li, J.M. Franssen, Test results and model for the residual compressive strength of concrete
665 after a fire, J. Struct. Fire Eng. 2 (2011) 29–44. https://doi.org/10.1260/2040-2317.2.1.29.

666 [38] Q. Ma, R. Guo, Z. Zhao, Z. Lin, K. He, Mechanical properties of concrete at high temperature-A
667 review, Constr. Build. Mater. 93 (2015) 371–383.
668 https://doi.org/10.1016/j.conbuildmat.2015.05.131.

669 [39] I.C. Neves, J.P.C. Rodrigues, A. De Pádua Loureiro, Mechanical properties of reinforcing and
670 prestressing steels after heating, J. Mater. Civ. Eng. 8 (1996) 189–194.
671 https://doi.org/10.1061/(ASCE)0899-1561(1996)8:4(189).

672 [40] Z. Tao, X.Q. Wang, B. Uy, Stress-strain curves of structural and reinforcing steels after exposure
673 to elevated temperatures, J. Mater. Civ. Eng. 25 (2013) 1306–1316.
674 https://doi.org/10.1061/(ASCE)MT.1943-5533.0000676.

675 [41] R. Felicetti, P.G. Gambarova, A. Meda, Residual behavior of steel rebars and R/C sections after
676 a fire, Constr. Build. Mater. 23 (2009) 3546–3555.
677 https://doi.org/10.1016/j.conbuildmat.2009.06.050.

678 [42] S. Reitgruber, C. Di Blasi, J. Franssen, Some Comments on the Parametric Fire Model of
679 Eurocode 1, Conf. Fire Enclosures. (2006) 1–25.

680 [43] C. Bucher, Computational Analysis of Randomness in Structural Mechanics, CRC Press, Vienna,
681 2009. https://doi.org/10.1201/9780203876534.

682 [44] R. Van Coile, D. Hopkin, L. Bisby, R. Caspeele, The meaning of Beta: Background and applicability
683 of the target reliability index for normal conditions to structural fire engineering, Procedia Eng.
684 210 (2017) 528–536. https://doi.org/10.1016/j.proeng.2017.11.110.

685 [45] R. Qureshi, S. Ni, N.E. Khorasani, R. Van Coile, T. Gernay, D. Hopkin, Probabilistic models for

temperature dependent strength of steel and concrete, J. Struct. Eng. 146 (2020).

[46] The Joint Committee on Structural Safety, Probabilistic Model Code - Part 3.10: Dimensions, JCSS, 2001. https://doi.org/10.1002/1616-8984(200011)8:1<215::AID-SEUP215>3.0.CO;2-D.

[47] M. Holicky, Reliability analysis for structural design, SUN MeDIA Stellenbosch, 2009.

[48] E.G. Choi, Y.S. Shin, The structural behavior and simplified thermal analysis of normal-strength and high-strength concrete beams under fire, Eng. Struct. 33 (2011) 1123–1132. https://doi.org/10.1016/j.engstruct.2010.12.030.

[49] B. Jovanović, R. Van Coile, D. Hopkin, N. Elhami Khorasani, D. Lange, T. Gernay, Review of Current Practice in Probabilistic Structural Fire Engineering: Permanent and Live Load Modelling, Fire Technol. (2020). https://doi.org/10.1007/s10694-020-01005-w.

Annex A: Regression model for maximum rebar temperature

Table A.1: Polynomial equations from regression model for maximum rebar temperatures Θ_{max}

Ventilation controlled fires	$\Theta(q_f,O,a)$ = 5.001E+02 - 1.450E+03*q_f + 5.489E-01*y - 1.073E+04*a + 3.869E-01*q_f*O - 4.963E+04*q_f*a - 3.553E+00*O*a + 8.728E+03*q_f^2 - 1.851E-04*O^2 + 1.419E+05*a^2 - 7.754E-01*q_f^2*O + 1.315E+05*q_f^2*a - 3.379E-06*O^2*q_f + 8.205E-04*O^2*a + 3.014E+05*a^2*q_f + 8.282E+00*a^2*O - 9.689E+00*q_f*O*a - 2.920E+04*q_f^3 + 2.565E-08*O^3 - 7.189E+05*a^3
Fuel controlled fires	$\Theta(q_f,O,a)$ = -9.618E+01 - 7.650E+02*q_f + 2.426E+00*O + 1.366E+03*a - 4.148E+00*q_f*O - 2.804E+03*q_f*a - 4.065E+01*O*a + 3.816E+03*q_f^2 - 2.432E-03*O^2 - 1.432E+03*a^2 + 2.030E+01*q_f^2*O - 1.783E+02*q_f^2*a - 3.517E-03*O^2*q_f + 1.521E-02*O^2*a - 2.852E+02*a^2*q_f + 3.747E+02*a^2*O + 4.528E+01*q_f*O*a + 1.364E+03*q_f^3 + 2.177E-06*O^3 - 1.638E+02*a^3 - 8.841E+01*q_f^3*O + 1.248E+01*q_f^3*a - 4.949E-06*O^3*q_f - 2.663E-06*O^3*a - 2.510E+01*a^3*q_f - 1.610E+03*a^3*O + 3.565E-02*q_f^2*O^2 - 2.854E+01*q_f^2*a^2 - 3.761E-02*O^2*a^2 - 6.878E+01*q_f^2*O*a - 1.793E-02*O^2*q_f*a - 1.308E+01*a^2*q_f*O + 3.442E+02*q_f^4 - 3.475E-10*O^4 - 1.448E+01*a^4